Available online at www.sciencedirect.com
ScienceDirect
Journal of Nutritional Biochemistry 22 (2011) 476–486
Journal of Nutritional Biochemistry

4-*O*-methylhonokiol attenuated β-amyloid-induced memory impairment through reduction of oxidative damages via inactivation of p38 MAP kinase☆

Yong Kyung Lee[a], Im Seop Choi[a], Jung Ok Ban[a], Hwa Jeong Lee[a], Ung Soo Lee[b], Sang Bae Han[a], Jae Kyung Jung[a], Young Hee Kim[c], Ki Ho Kim[c], Ki-Wan Oh[a], Jin Tae Hong[a,*]

[a]*College of Pharmacy and MRC, Chungbuk National University, Heungduk-gu, Cheongju, Chungbuk 361-763, South Korea*
[b]*Department of Food and Biotechnology, Chungju National University, Iryu-myeon, Chungju, Chungbuk 380-702, South Korea*
[c]*R&D Center, Bioland Ltd., Songjeong, Byongchon, Cheonan-Si, Chungnam 330-863, South Korea*

Received 24 October 2009; received in revised form 4 April 2010; accepted 5 April 2010

Abstract

Oxidative stress induced neuronal cell death by accumulation of β-amyloid (Aβ) is a critical pathological mechanism of Alzheimer's disease (AD). Intracerebroventrical infusion of $A\beta_{1\text{-}42}$ (300 pmol/day per mouse) for 14 days induced neuronal cell death and memory impairment, but pre-treatment of 4-*O*-methylhonokiol (4-*O*-MH), a novel compound extracted from *Magnolia officinalis* for 3 weeks (0.2, 0.5 and 1.0 mg/kg) prior to the infusion of $A\beta_{1\text{-}42}$ and during the infusion dose dependently improved $A\beta_{1\text{-}42}$-induced memory impairment and prevented neuronal cell death. Additionally, 4-*O*-MH reduced $A\beta_{1\text{-}42}$ infusion-induced oxidative damages of protein and lipid but reduced glutathione levels in the cortex and hippocampus. $A\beta_{1\text{-}42}$ infusion-induced activation of astrocytes and p38 mitogenic activated protein (MAP) kinase was also prevented by 4-*O*-MH in mice brains. In further study using culture cortical neurons, p38 MAP kinase inhibitor abolished the inhibitory effect of 4-*O*-MH (10 μM) on the $A\beta_{1\text{-}42}$ (5 μM)-induced reactive oxidative species generation and neuronal cell death. These results suggest that 4-*O*-MH might prevent the development and progression of AD through the reduction of oxidative stress and neuronal cell death via inactivation of p38 MAP kinase pathway.

Keywords: 4-*O*-MH; β-amyloid; p38 MAP kinase; Alzheimer's disease

1. Introduction

Alzheimer's disease (AD) is the most common neurodegenerative disease of the brain. AD is characterized by intraneuronal neurofibrillary tangle and cerebral parenchyma deposition of the amyloid beta peptide (Aβ) [1]. Aβ peptide is thought to be a critical factor in AD pathogenesis, and this peptide is derived from amyloid precursor protein by series of proteolysis process [2–4]. Aβ abnormally accumulates in the brains of patients with AD, and can increase loss of neuronal cells due to induced neuronal cell death [4–8].

Activation of mitogen-activated protein kinase (MAP kinase) pathway is important in the neuronal cell death against various damages [9–11]. In several studies, it has been suggested that inhibition of MAP kinases signals could contribute to the decreased neuronal cell death caused by Aβ [12–14]. Previously, we demonstrated that reduction of MAP kinases signals protected neuronal cell death induced by Aβ [15] and inhibition of MAP kinase signals by neuroprotective compounds such as eigallocatechin 3′-gallate (EGCG) which showed a preventive effect against Aβ-induced neuronal cell death in the development of AD [16,17]. Oxidative stress is also a well-known event in the pathogenesis of AD and Aβ-induced neuronal cell death pathway [18–20]. Aβ causes neuronal cell death by the impairment of mitochondrial activity [18,21,22] and activation of other series cell death pathway cascades [23] through the induction of reactive oxygen species (ROS). Therefore, antioxidants could act to prevent or inhibit neuronal damages in the brains of AD. Many studies have been reported that compounds having antioxidant effects might prevent neuronal cell death against various damages [24,25] and prevent progression of AD [26,27]. Our previous studies showed that natural compounds such as theanine and EGCG have anti-oxidative properties which protect from Aβ-induced neuronal cell death and memory impairment [16,28].

The bark of the root and stem of *Magnolia* family has been used in traditional medicine to treat various disorders [29,30]. Several compounds isolated from *Magnolia* family such as honokiol, obovatol and magnolol have anti-inflammatory [31–33], neuroprotective effects [24,25] and anti-oxidative effects [34,35]. A recent study found that honokiol exhibited neuroprotective effect by preserving mitochondrial activity on ischemia-induced neuronal damage [36]. Recently, we isolated 4-*O*-methylhonokiol (4-*O*-MH), a novel

☆ Grants: This work was supported by the Korea Research Foundation Grant (MRC, 2009-0091433) and by the Research Grant from Bioland (Chungnam, Korea).
* Corresponding author. College of Pharmacy, Chungbuk National University, Heungduk-gu, Cheongju, Chungbuk 361-763, South Korea. Tel.: +82 43 261 2813; fax: +82 43 268 2732.
E-mail address: jinthong@chungbuk.ac.kr (J.T. Hong).

0955-2863/$ - see front matter © 2011 Elsevier Inc. All rights reserved.
doi:10.1016/j.jnutbio.2010.04.002

compound from *Magnolia officinalis,* and found that it exhibited anti-inflammatory [37] and neurotropic activity [38]. Moreover, we demonstrated that the ethanol extract of *M. officinalis* had a memory improving effect of 4-*O*-MH on the scopolamine-induced memory deficiency animal model [39] as well as $A\beta_{1-42}$ single injection mice memory deficiency model (unpublished data). Thus, we investigated the protective effect of 4-*O*-MH on the continued infusion of $A\beta_{1-42}$-induced memory impairment and neuronal cell death and the underlying mechanisms of memory improving effects.

2. Materials and methods

2.1. 4-O-MH

4-*O*-MH was isolated and identified from the bark of *M. officinalis* as described elsewhere [37,38]. 4-*O*-MH (purity; more than 99.5%) was dissolved in 0.05% ethanol and added to drinking water where mice were allowed access ad libitum. The structure is shown in Fig. 1.

2.2. $A\beta_{1-42}$-infused Alzheimer's disease mouse model

Eight-weeks-old male mice Slc:ICR (Central Lab. Animal, Seoul, Korea) were maintained in accordance with the National Institute of Toxicological Research of the Korea Food and Drug Administration guidelines as well as the regulations for the care and use of laboratory animals of the animal ethics committee of Chungbuk National University. All mice were housed in a room that was automatically maintained at 21–25°C and relative humidity (45–65%) with a controlled light–dark cycle. The infusion model was adapted from previous work on the rat infusion model [40,41]. The anesthetized animals were placed in a sterotaxic instrument, and catheters were attached to an osmotic mini-pump (Alzet 2001, ALZA, Mountain View, CA, USA) which were implanted according to the following coordinates: mouse (unilaterally): −1.0 mm anterior/posterior, +1.0 mm medial/lateral and −2.5 mm dorsal/ventral. The pump contents were released over a period of 14 days consisting of 300 pmol aggregated $A\beta_{1-42}$ (purity 97.1%, Sigma Chemical, St. Louis, MO, USA) dissolved in sterile saline (0.9% NaCl) for each pump.

2.3. Water maze test

The water maze test is a widely accepted method for memory test, thus we performed this test as the method to induce memory impairment as described by Morris et al. [42]. Maze testing was performed by the SMART-LD program and equipment (Panlab, Barcelona, Spain). A circular plastic pool (height: 35 cm, diameter: 100 cm) was filled with water (within dark ink) kept at 22–25°C. An escape platform (height: 14.5 cm, diameter: 4.5 cm) was submerged 0.5–1 cm below the surface of the water in position. Test was performed three times per day for 7 days. Each trial lasted for 60 s or ended as soon as the mice reached the submerged platform and remained on the platform for 10 s. Mice were allowed to swim until they sought the escape platform. Escape latency, escape distance, swimming speed and swimming pattern of each mouse was monitored by a camera above the center of the pool connected to a SMART-LD program. A quiet environment, consistent lighting, constant water temperature and fixed spatial frame were maintained throughout the period of the experiment.

2.4. Probe test

A probe trial in order to assess memory consolidation was performed 24 h after the 7-day acquisition tests. In this trial, the platform was removed from the tank, and the mice were allowed to swim freely. For these tests, the percentage time in the target quadrant and target site crossings within 60 s was recorded. The time spent in the target quadrant is taken to indicate the degree of memory consolidation that has taken place after learning. The time spent in the target quadrant was used as a measure of spatial memory. Swimming pattern of each mouse was monitored by a camera above the center of the pool connected to a SMART-LD program as described above.

2.5. Passive avoidance performance test

The passive avoidance test is also a widely accepted simple and rapid method for memory test. The passive avoidance response was determined using a "step-through" apparatus (Med Associates, Georgia, VT, USA) that is consisted of an illuminated and a dark compartment (each 20.3×15.9×21.3 cm) adjoining each other through a small gate with a grid floor, 3.175 mm stainless steel rod set 8 mm apart. One day after the water maze test, training trial was performed. The ICR mice were placed in the illuminated compartment facing away from the dark compartment. When the mice moved completely into the dark compartment, it received an electric shock (1 mA, 3-s duration). The mice were then returned to their home case. At 1 day later, the mice were placed in the illuminated compartment and the latency period to enter the dark compartment defined as "retention" was measured. The time when the mice entered in the dark compartment were recorded and described as step-through latency. The retention trials were set at a limit of 180 s as the cutoff time.

2.6. Brain tissue collection and preservation

After the behavioral test (step through test), animals were perfused with phosphate-buffered saline (PBS) under inhalated chloroform anesthetization. The brains were immediately collected in the same manner and frozen stored at −20°C and separated into cortical and hippocampal regions. All the brain regions were immediately stored at −80°C and used to measure biological assay of $A\beta_{1-42}$ and cell death detection.

2.7. Western blotting

Cells and each area of the brain tissue were homogenized with lysis buffer [50 mM Tris pH 8.0, 150 mM sodium chloride (NaCl), 0.02% sodium azide, 0.2% sodium dodecyl sulfate (SDS), 1 mM phenylmethanesulphonylfluoride or phenylmethylsulphonyl fluoride, 10 μl/ml aprotinin, 1% igapel 630, 10 mM sodium fluoride, 0.5 mM

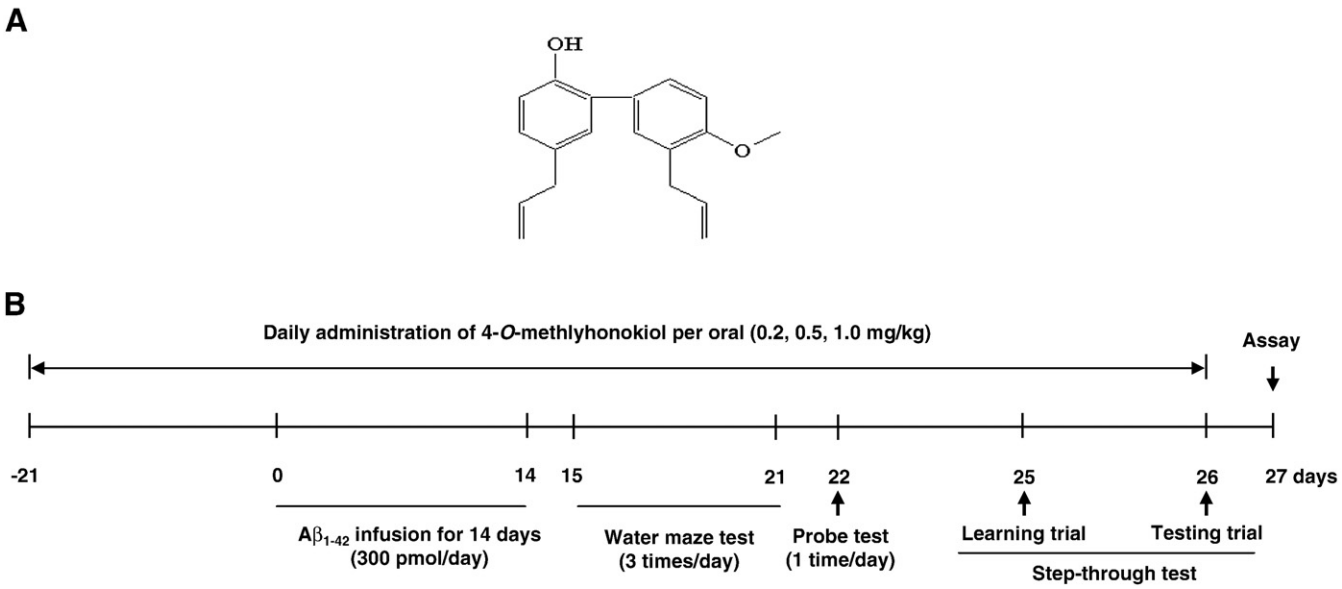

Fig. 1. Chemical structure of 4-*O*-MH (A) and Experimental scheme (B).

ethylenediaminetetraacetic acid (EDTA), 0.1 mM ethylene glycol tetraacetic acid and 0.5% sodium deoxycholate], and centrifuged at 15,000×*g* for 15 min. Equal amount of proteins (40 μg) were separated on a SDS/10 and 15% polyacrylamide gel and then transferred to a nitrocellulose membrane (Hybond ECL, Amersham Pharmacia Biotech, Piscataway, NJ, USA). Blots were blocked for 2 h at room temperature with 5% (w/v) nonfat dried milk in Tris-buffered saline [10 mM Tris (pH 8.0) and 150 mM NaCl] solution containing 0.05% tween-20. The membrane was then incubated for 3 h at room temperature with specific antibodies. Rabbit polyclonal antibodies against active form of JNK1 (1:500), ERK2 (1:500) and p38 MAP kinase (1:500), mouse polyclonal antibodies against phosphorylation forms of JNK1 (1:500), ERK2 (1:500) and p38 MAP kinase (1:500) (Santa Cruz Biotechnology, Santa Cruz, CA, USA) were used in this study. The blots were then incubated with the corresponding conjugated anti-rabbit, anti-mouse and anti-goat immunoglobulin G-horseradish peroxidase (Santa Cruz Biotechnology). Immunoreactive proteins were detected with the ECL Western blotting detection system. The relative density of the protein bands was quantified by densitometry using Electrophoresis Documentation and Analysis System 120 (Eastman Kodak Com., Rochester, NY, USA).

2.8. Immunohistochemistry

Mice were anesthetized with ether. While under general anesthesia, the mice received intracardiac perfusion with 20 ml of saline, followed by 50 ml of PBS containing 4% paraformaldehyde. After perfusion, the brains and spinal cords were dissected and post-fixed for 2–4 h in the same fixative and were then cryoprotected overnight in 30% sucrose prepared in PBS. Serial coronal sections of the brain and spinal cord (40 μm) were cut with a freezing microtome. Immunohistochemical staining was performed using the avidin-biotin peroxidase method. The sections were incubated overnight at 4°C with anti-A$\beta_{1\text{-}42}$ (NAB228; 1:2000, Covance, Berkely, CA, USA). After washing in PBS, the sections were incubated in biotinylated goat anti rabbit IgG (1:2000 dilution, Vector Laboratories, Burlingame, CA, USA) for 1 h at room

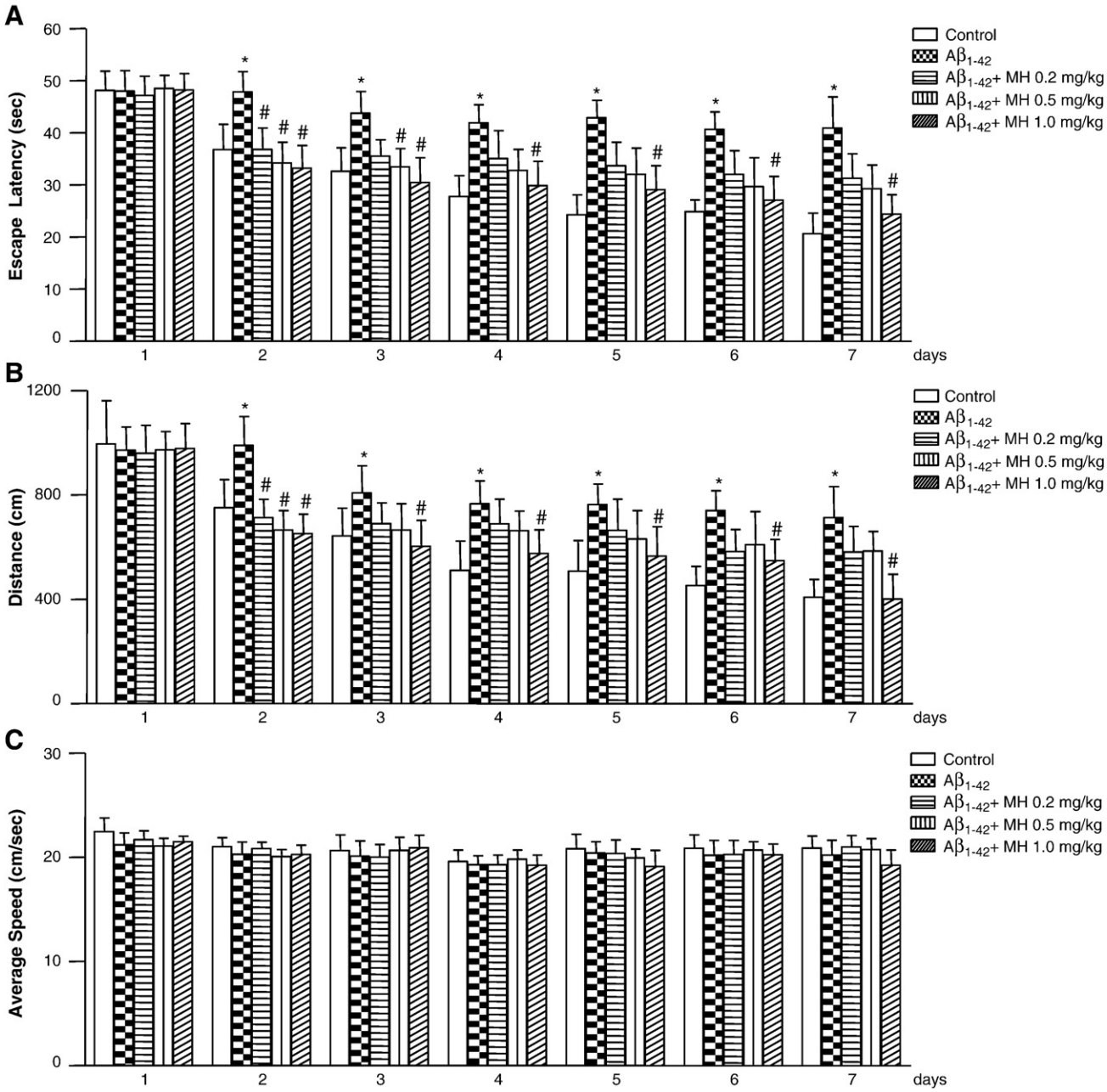

Fig. 2. Inhibitory effect of 4-*O*-MH on A$\beta_{1\text{-}42}$-induced memory impairment determined with water maze test. Mice were treated with i.c.v. infusion of A$\beta_{1\text{-}42}$ (300 pmol per mouse) after 3 weeks treatment of. 4-*O*-MH. Training trial was done for two day, test trials were then performed once a day for five days. Swimming time (A), swimming distance (B) and average speed (C) to arrive at the location of the platform was recorded. Values are presented as mean±S.E. from 10 mice. *Significant difference from untreated control (P<.05). #Significantly different from A$\beta_{1\text{-}42}$-treated control (P<.05).

temperature. The sections were subsequently washed and incubated with avidin-conjugated peroxidase complex (ABC kit, 1:200 dilution, Vector Laboratories) for 30 min followed by PBS washing. The peroxidase reaction was performed in PBS using 3,3′-diaminobenzidine tetrahydrochloride (0.02%) as the chromogen. Finally, the sections were rinsed, mounted on poly-glycine-coated slides, dehydrated and cover-slipped for light microscopy and photography.

2.9. Detection of apoptosis

DNA fragmentation was examined by terminal deoxynucleotydyl trasferase-mediated FITC-dUDP nick-end labeling (TUNEL). TUNEL assays were performed by using the in situ Cell Death Detection Kit (Roche Diagnostics, Mannheim, Germany) according to the manufacturer's instructions. Briefly, after the fixation of 40 μm cryosections with 4% paraformaldehyde and treatment with 0.1% NaBH4 and 0.1% Triton X-100, the slides were incubated at least for 1 h with a reaction mix containing deoynucleotidyl trasferase and FITC-dUDP (Roche, Reinach, Switzerland). For 4′-6′-diamidino-2-phenylindole digydrochloride (DAPI) staining slides were incubated for 15 min at room temperature in the dark with mounting medium for fluorescence containing DAPI (Vector Laboratories). The tissues were then observed through a fluorescence microscope (Leica Microsystems, Wetzlar, Germany). Staining the nuclei was visualized using DAPI.

2.10. Determination of carbonyl protein levels for oxidative protein product

Protein carbonyls in brain tissue were measured using the Cayman Protein Carbonyl assay kit (Cayman Chemical, Ann Arbor, MI, USA), according to the manufacturer's instructions. In brief, 0.1 g of brain tissue was homogenized with 1 ml of 50 mM 2-(*N*-morpholino)ethanesulphonic (MES) containing 1 mM EDTA. After centrifugation at 10,000×*g* for 15 min at 4°C, 200 μl of supernatant of each sample was transferred to two 2-ml plastic tubes: a sample tube and a control tube. Eight hundred microliters of 10 mM 2,4-dinitrophenylhydrazine (DNPH) was added to the sample tube and 800 μl of 2.5 M hydrogen chloride to the control tube and then incubated in the dark at room temperature for 1 hr with vortexing every 15 min. One milliliter of 20% trichloroacetic acid (TCA) was added to each tube, vortexed and incubated on ice for 5 min. After centrifugation for 10 min at 10,000×*g*, the supernatant was discarded and the pellet was resuspended with 1 ml of 10% TCA and incubated on ice for 5 min. After centrifugation for 10 min at 10,000×*g*, the pellets were washed with 1 ml of ethanol-ethyl acetate (1:1) mixture to remove any unreacted DNPH. After repeating the wash three times with 1 ml of ethanol-ethyl acetate (1:1) mixture, the pellets were solubilized with 500 μl of guanidine hydrochloride and centrifuged at 10,000×*g* for 10 min at 4°C to remove insoluble material. Carbonyl content was calculated from the absorbance measurement at 385 nm using a microplate absorbance reader (Molecular Devices, Sunnyvale, CA, USA) and expressed as nmol/mg of protein.

2.11. Measurement of lipid peroxidation product

As a measure of lipid peroxidation, the levels of hydroxynonenal–histidine (HNE–His) protein adducts in brain tissue were quantified by using the Oxiselect HNE–His Adduct ELISA Kit (Cell Biolabs, San Diego, CA, USA), according to the manufacturer's instructions. In brief, 0.5 g of brain tissue was homogenized with 1 ml of PBS containing 1% triton X-100. One hundred microliters of the 2 mg/ml protein sample was transferred to a 96-well protein binding plate, incubated for 4°C overnight and washed 2 times with 250 μl of 1× PBS per well. Two hundred microliters of Assay per well was added to the 96-well protein binding plate, incubated for 2 h at room temperature on an orbital shaker and washed three times with 250 μl of 1× wash buffer per well. One hundred microliters of the diluted anti-HNE–His antibody solution was added to all wells, incubated for 1 h at room temperature on the orbital shaker and washed again with 250 μl of 1× wash buffer per well. One hundred microliters of the secondary antibody–horseradish peroxidase (HRP) conjugate solution was added to all wells, incubated for 1 h at room temperature on the orbital shaker and washed again with 250 μl of 1× wash buffer per well. After the final wash, 100 μl of substrate solution (tetramethylbenzidine [TMB]) was added to each well and incubated for 20 min at room temperature. One hundred microliters of stopping reagent (0.5 M sulfuric acid) was added, and then HNE–His protein adduct was calculated from the absorbance measurement at 450 mm using a microplate absorbance reader (Sunrise, Tecan, Switzerland) absorbance reader and expressed as pmol/mg of protein.

2.12. Measurement of total glutathione level

Total glutathione levels in brain tissue were determined using a glutathione assay kit (Cayman Chemical, Ann Arbor, MI, USA) according to the manufacturer's instructions. In brief, 0.1 g of brain tissue was homogenized with 1 ml of 50 mM MES containing 1 mM EDTA. After centrifugation for 15 min at 10,000×*g*, 1 ml of 10% metaphosphoric acid was added to the 1 ml of supernatant for deproteination, vortexed and incubated for 5 min at room temperature. After centrifugation for 2 min at 2,000×*g*, 50 μl of 4 M triethanolamine (Sigma) per ml of supernatant was added to each sample. Fifty microliters of sample was transferred to a 96-well plate and 150 μl of assay cocktail [MES Buffer (11.25 ml)], reconstituted Cofactor Mixture (0.45 ml), reconstituted enzyme mixture (2.1 ml), water (2.3 ml) and reconstituted 5,5'-dithiobis (2-nitrobenzoic acid); DTNB (0.45 ml), was added to each well. After incubation for 30 min at room temperature, the glutathione (GSH) levels were calculated from the absorbance measurement at 405-nm microplate absorbance reader (Sunrise, Tecan, Switzerland) and expressed as nmol/mg of protein.

2.13. Cortical neuronal cell culture

Cortical neuronal cells were incubated with $A\beta_{1\text{-}42}$ in the absence or presence of 4-*O*-MH dissolved in 0.05% ethanol for 48 h for viability, expression of apoptotic or apoptotic signal proteins and apoptotic assay and for 4 h for reactive oxygen species. Cultures of dissociated cortical cells were prepared from Day 18 embryos of ICR mice pups using methods similar to those previously described [8]. Briefly, cerebral cortices were removed and incubated for 15 min in Ca^{2+}- and Mg^{2+}-free Hanks' balanced saline solution (Life Technologies, Carlsbad, CA, USA) containing 0.2% trypsin. Cells were dissociated by trituration and plated into polyethyleneimine-coated plastic or glass-bottom culture dishes containing minimum essential medium with Earle's salts supplemented with 10% heat-inactivated fetal bovine serum, 2 mM L-glutamine, 1 mM pyruvate, 20 mM KCl, 10 mM sodium bicarbonate and 1 mM Hepes (pH 7.2). Following cell attachment (3–6 h after plating), the culture medium was replaced with neurobasal medium containing B27 supplements (Life Technologies). Experiments were performed with 6- to 8-day-old cultures; greater than 90% of the cells in these cultures were neurons, and the remainder were astrocytes, as judged by cell morphology and by immunostaining with antibodies against neurofilaments and glial fibrillary acidic protein. For calcium measurements, cortical neuronal cells were isolated from 1-day-old mice brains, and intracellular calcium levels were immediately determined.

2.14. Cell viability

The cells were plated in 96-well plates, and cell viability was determined by the conventional 4-(3-(4-Iodophenyl)-2-(4-nitrophenyl)-2H-5-terazolio)-1,3-benzene disulfonate (WST-1) reduction assay (Dojin Laboratory, Kumanoto, Japan). WST-1 assay measures the activity of intramitochondrial and extramitochondrial dehydrogenases. Briefly, tetrazolium salts are cleaved by dehydrogenases of viable cells to produce formazan and the change of absorbance is detected spectrophotometrically. The cells were exposed with $A\beta_{1\text{-}42}$ (5 μM) with/without various concentrations of 4-*O*-MH (10

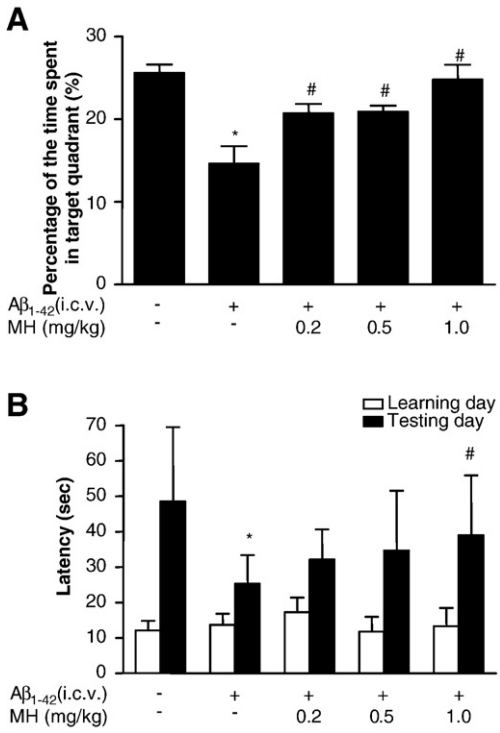

Fig. 3. Inhibitory effect of 4-*O*-MH on $A\beta_{1\text{-}42}$-induced memory impairment determined with step-through type passive avoidance performance test. (A) One day after test trials, a probe test was performed. Shown is representative swim paths in a probe test conducted following the completion of training. (B) One day after water maze test mice, the mice were given electric shock when entered dark room for training trial. One day of the trial, the retention time in white box was recorded. Values are presented as mean±S.E. from 10 mice. *Significant difference from untreated control ($P<.05$). #Significantly different from $A\beta_{1\text{-}42}$-treated control ($P<.05$).

μM) for 24 h to examine the recovery effect of 4-*O*-MH on $A\beta_{1-42}$-induced killing of the cells. The cells were treated with the WST-1 solution (final concentration, 1 mg/ml) for 2 h. The absorbance was measured with a microplate reader (Tecan, sunrise, Salzburg, Austria) at 450 nm. Results were expressed as the percentage of WST-1 reduction.

2.15. ROS generation

To monitor intracellular accumulation of ROS, the fluorescent probe 2′,7′-dichlorofluorescein diacetate (DCF-DA) was used. Following treatment with $A\beta_{1-42}$ (5 μg/ml) for 24 h in the presence or absence of 4-*O*-MH (10 μM), the cells were washed in modified Kreb's buffer containing 145 mM NaCl, 5 mM potassium chloride (KCl), 1 mM magnesium chloride ($MgCl_2$), 1 mM calcium chloride (CaCl2), 4 mM sodium hydrogen carbonate (NaHCO3), 5.5 mM glucose, 10 mM Hepes, pH 7.4. The cell suspension was transferred into plastic tubes. Measurement was started by an injection of 5 μM DCF-DA in the dark. After 30 min of incubation at 37°C, generation was determined by Fluorometer (fmax, Molecular Devices, San Diego, CA, USA) at Ex=485 and Em=538 nm.

2.16. Statistical analysis

Statistical analysis of the data was carried out using analysis of variance (ANOVA) for repeated measures followed by Dunnette's post hoc analysis using GraphPad Prism 4 software (Version 4.03, GraphPad software).

3. Results

3.1. Effect of 4-O-MH on $A\beta_{1-42}$-induced memory impairment

To investigate the effect of 4-*O*-MH on $A\beta_{1-42}$ infusion-induced memory impairment, we performed the passive avoidance test

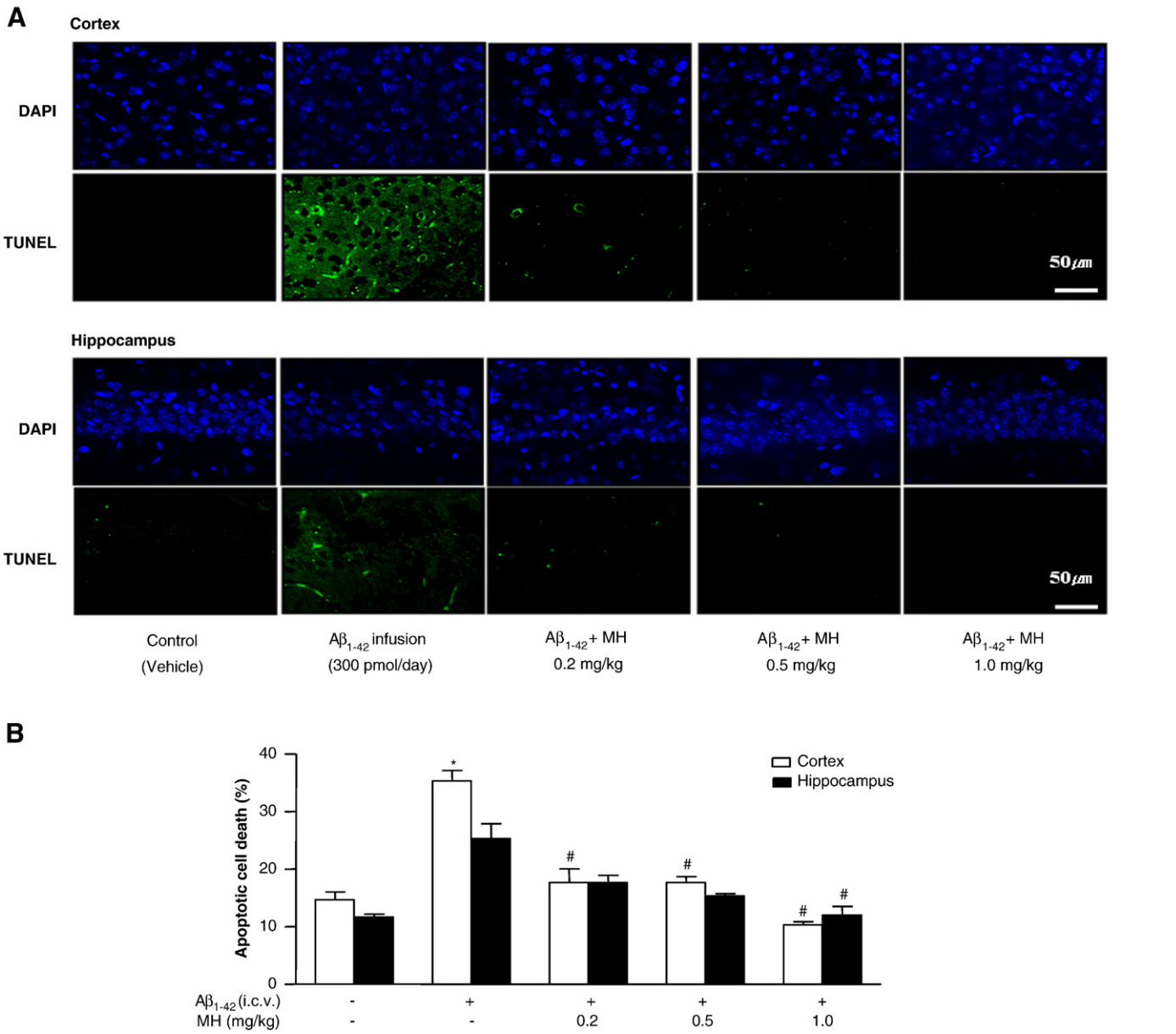

Fig. 4. Inhibitory effect of 4-*O*-MH on the $A\beta_{1-42}$-induced apoptotic cell death. (A) The mice were continuously treated with the oral administration of 4-*O*-MH (0.2, 0.5 and 1.0 mg/kg) for 3 weeks. The brain section was washed twice with PBS and fixed by incubation in 4% paraformaldehyde for 1 h at room temperature. TUNEL assays were performed using the in situ Cell Death Detection Kit (Roche Diagnostics GmbH, Mannheim, Germany) according to the manufacturer's instructions. For the DAPI staining, slides were incubated 30 min at room temperature in the dark with mounting medium for fluorescence containing DAPI (Vector Laboratories, Burlingame, CA, USA). The tissue sections were then observed through a fluorescence microscope (Leica Microsystems, Wetzlar, Germany). (B) Total number of cells in a given area was determined by using DAPI nuclear staining. The apoptotic index was determined as the number of TUNEL-positive stained cells divided by the total cell number counted×100. The apoptotic cells were examined by morphologic analysis, DAPI staining and TUNEL assay. *Significantly different from vehicle control ($P<.05$). #Significantly different from $A\beta_{1-42}$-treated control ($P<.05$).

(step-through test) and the Morris water maze. 4-*O*-MH (0.2, 0.5 and 1 mg/kg) was orally administered for 3 weeks prior to Aβ infusion and during the infusion (300 pmol/day, 2 weeks). The animals were then trained for three trials per day for 2 days, and their last spatial learning scores (latency in seconds and in length) were recorded (Days 1 and 2 in the Fig. 2). The mice were then tested for 5 consecutive days to locate and escape onto the platform, and their spatial learning scores were also recorded (Days 3–7 in Fig. 2). The control mice exhibited shorter escape latency with the training, however, the escape latency of $A\beta_{1\text{-}42}$-infused mice was not significantly reduced compared to the control mice. In contrast, the 4-*O*-MH-treated groups significantly inhibited the effects of $A\beta_{1\text{-}42}$ on escape latencies (cm and s) in a dose-dependent manner (Fig. 2). Statistical analysis (ANOVA) of data on Day 7 showed the significance of a memory improving effect with 1 mg 4-*O*-MH treatment [escape latency $F(4,287)=10.32$, $P<.00001$; escape distance, $F(4,287)=5.30$, $P<.0004$]. However, there was no difference on average speed between $A\beta_{1\text{-}42}$ and 4-*O*-MH treated groups [$F(4,287)=0.5355$, $P<.05$] (Fig. 2C). After the water maze test, we performed a probe trial to measure the maintenance of memory. During the probe trial, the time spent on the target quadrant of $A\beta_{1\text{-}42}$-induced group was reduced compared to the control group. This impairment of memory maintenance was prevented by 4-*O*-MH treatment, and one-way ANOVA analysis revealed significant difference between $A\beta_{1\text{-}42}$ and 4-*O*-MH treated groups [$F(3,28)=7.184$, $P=.0012$] (Fig. 3A). We also evaluated learning and memory capacities by the passive avoidance test through the step-through method. In the passive avoidance test, there was no significant difference on the learning trial. However, infusion of $A\beta_{1\text{-}42}$ significantly decreased the step-through latency compared to the control group (vehicle), and this memory impairment was prevented by 4-*O*-methlyhonokiol treatment. The control group exhibited step-through latency about 48.5±20.9 s, whereas the $A\beta_{1\text{-}42}$-induced group was decreased to 25.3±8.1 s [$F(1,8)=5.990$, $P=.2969$]. The 4-*O*-MH-treated groups were increased to 32.1±8.5 s (0.2 mg/kg) [$F(1,8)=1.2349$, $P=.5716$], 34.7±16.9 s (0.5 mg/kg) [$F(1,8)=4.342$, $P=.6219$] and 39.0±16.9 s (1.0 mg/kg) [$F(1,8)=4.882$, $P=.489$], respectively (Fig. 3B).

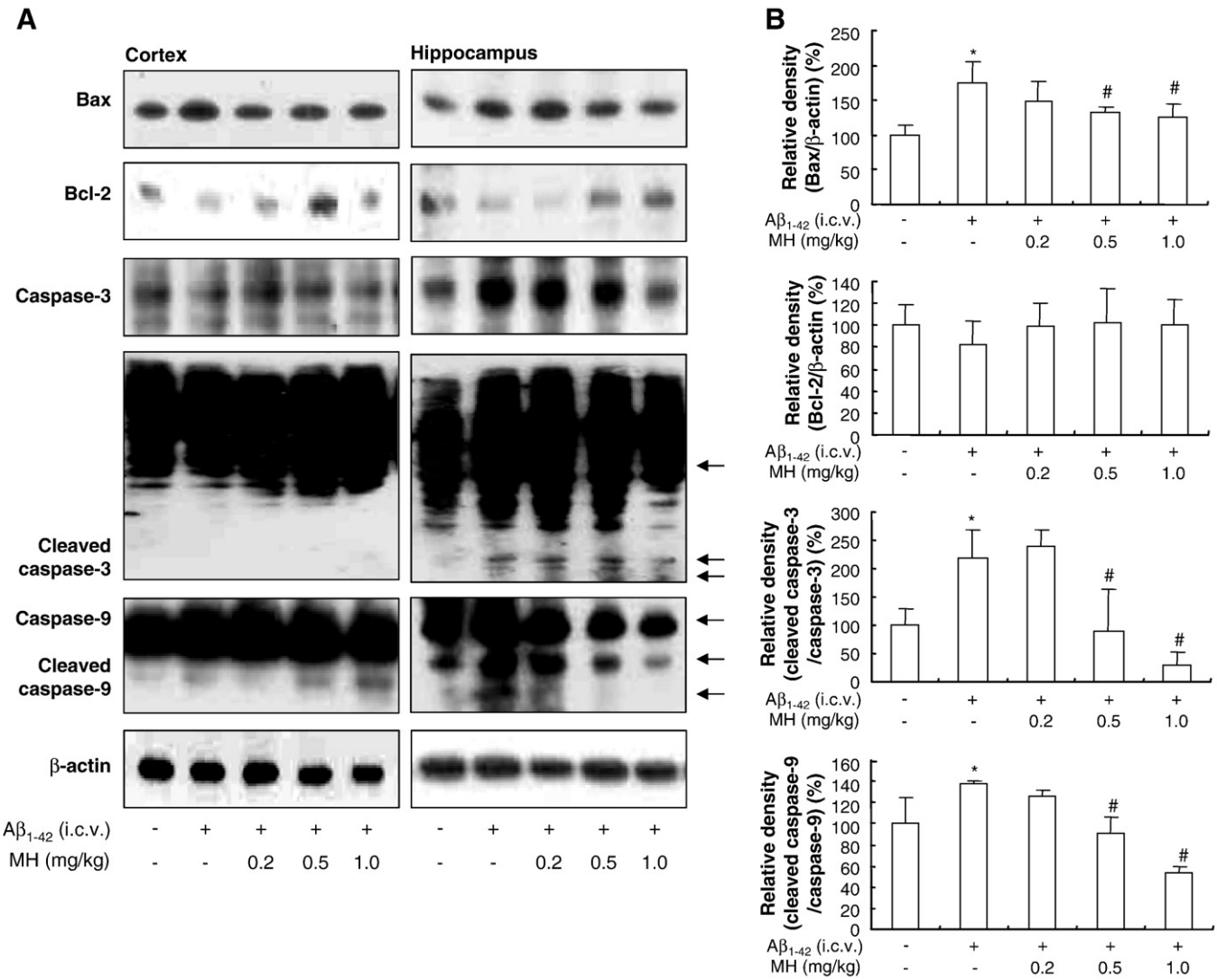

Fig. 5. Reversal effect of 4-*O*-MH on the $A\beta_{1\text{-}42}$-induced expression of apoptosis regulatory proteins. (A) Immunoblots of lysates from brain tissue were probed with apoptosis regulatory protein antibodies, respectively. Experiments were performed from three mice brains. β-actin levels were measured for the confirmation of equal amount of protein loading. (B) Densitometric values are the means±S.E. from three mice brains. *Significantly different from vehicle control ($P<.05$). #Significantly different from $A\beta_{1\text{-}42}$ treated control ($P<.05$).

3.2. Effect of 4-O-MH on $A\beta_{1-42}$-induced neuronal cell death

Neuronal cell death is a major causing factor in the development of AD. To examine the effect of 4-*O*-MH on $A\beta_{1-42}$-induced neuronal cell death, we measured whether 4-*O*-MH prevented $A\beta_{1-42}$-induced neuronal cell death. Infusion of $A\beta_{1-42}$ for 14 days led to a significant increase of neuronal cell death compared to the control group (35.3% versus 14.41%), which was prevented by 4-*O*-MH. The percentage of apoptotic cell death was down to 17.5, 17.4% and 10.5 by 0.2, 0.5 and 1.0 mg/kg 4-*O*-MH in the cortex. In the hippocampus, $A\beta_{1-42}$ infusion increased apoptotic cell death compared to the control group (25.1% versus 11.9%), which was inhibited to 17.9%, 15.4% and 12.0% by 0.2, 0.5 and 1.0 mg/kg 4-*O*-MH treatment (Fig. 4A and B). In addition, we performed a western blot to investigate the expression of apoptotic and anti-apoptotic proteins. The brains of $A\beta_{1-42}$-infused animals showed increased expression of pro-apoptotic proteins (Bax, cleavage caspase 3 and 9) and decreased expression of anti-apoptotic protein Bcl-2. Pre-treatment of 4-*O*-MH increased the expression of Bcl-2 and decreased the expression of Bax and cleavage caspase 3 and 9 in the brains (Fig. 5).

3.3. Effect of 4-O-MH on astrocyte activation

Activation of astrocytes is implicated in the $A\beta_{1-42}$-induced neuronal cell death in the development of AD. To investigate the preventive effect of 4-*O*-MH on the astrocyte activation, we performed an immunohistochemical analysis of glial fibrillary acidic protein (GFAP) reactive cell number in the brain. Infusion of $A\beta_{1-42}$ led a significant elevation of GFAP reactive cell number, whereas the treatment of 4-*O*-MH reduced the number in the cortex and hippocampus in a dose-dependent manner (Fig. 6).

3.4. Effect of 4-O-MH on $A\beta_{1-42}$-induced glutathione, lipid peroxidation products and carbonyl protein levels

To investigate the neuroprotective effect of 4-*O*-MH through anti-oxidative properties, we evaluated glutathione levels and products of lipid peroxidation and carbonyl protein. The glutathione levels were decreased in the brains of $A\beta_{1-42}$-infused mice; however, the decreased glutathione levels were recovered by 4-*O*-MH treatment in a dose-dependent manner (Fig. 7A). The levels of 4-hydroxynonenal (HNE–His), a lipid peroxidation product, were

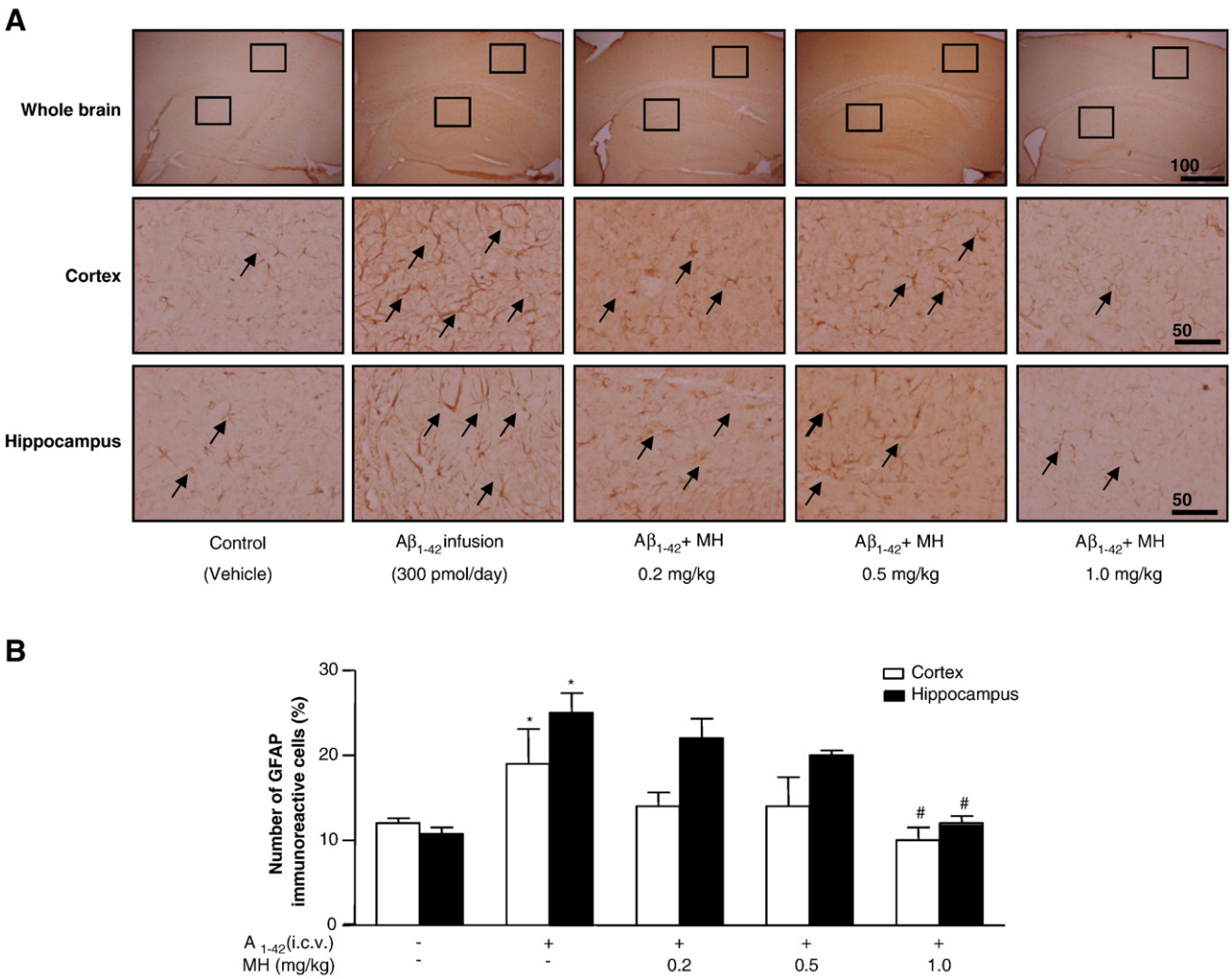

Fig. 6. Inhibitory effect of 4-*O*-MH on the $A\beta_{1-42}$-induced expression of GFAP. (A) One day after the step through test, immunostaining of GFAP in the cortex and hippocampus was performed 40 μm-thick sections of brains from mice were incubated with anti-GFAP primary antibodies and the biotinylated secondary antibody. It was then counterstained by a hematoxylin. The resulting tissue was viewed with a microscope. A representative sample from each group was stained in the picture. (B) The graph represents the number of GFAP immunoreactive cells in the mice brain. All values are the means±S.E. from three mice brains. *Significantly different from vehicle control ($P<.05$). #Significantly different from $A\beta_{1-42}$ treated control ($P<.05$).

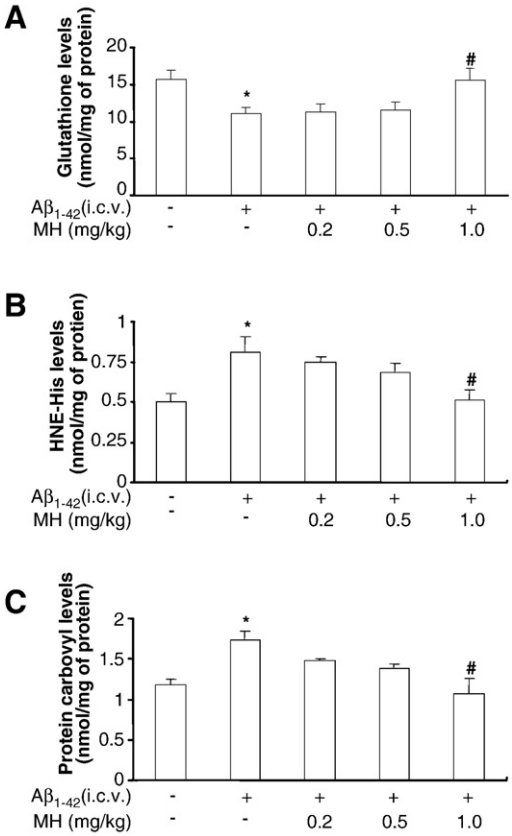

Fig. 7. Inhibitory effect of 4-*O*-MH on the $A\beta_{1\text{-}42}$-induced oxidative damages. Oxidative stress was determined by measuring (A) the levels of glutathione depletion and generation of (B) lipid peroxidation and (C) carbonyl protein in the brain of mice treated with 4-*O*-MH (0.2, 0.5 and 1.0 mg/kg). Values are presented as means±S.E. from three mice brains. *Significantly different from vehicle control ($P<.05$). #Significantly different from $A\beta_{1\text{-}42}$ treated control ($P<.05$).

increased by the infusion of $A\beta_{1\text{-}42}$. Treatment of 4-*O*-MH reduced lipid peroxidation products in a dose dependent manner (Fig. 7B). The carbonyl protein levels were also increased in the brains of $A\beta_{1\text{-}42}$-infused mice which was dose dependently reduced by 4-*O*-MH treatment (Fig. 7C).

3.5. Effect of 4-O-MH on $A\beta_{1\text{-}42}$-induced p38 MAPK activity

Since it is known that the activation of various MAP kinases is related with in oxidative stress and neuronal cell death, we examined the activation of MAPK in the brain. Infusion of $A\beta_{1\text{-}42}$ for 14 days increased activation of phosphorylation of p38 MAP kinase compared to the control group. However, pretreatment of 4-*O*-MH dose dependently decreased the expression of phosphorylated p38 MAP kinase as determined by Western blotting (Fig. 8A) as well as immunohistochemical analysis (Fig. 8B) in the cortex and hippocampus, but $A\beta_{1\text{-}42}$-induced activation of c-Jun N-terminal kinase (JNK) and extracellular signal-regulated kinase (ERK) was not changed by 4-*O*-MH treatment (data not shown). To elucidate a more precise mechanism of the involvement of p38 MAP kinase pathway in the protective effect of 4-*O*-MH on neuronal cell death, we also determined the p38 MAP kinase in the cultured cortical neuron. Correlated with the cell viability, p38 MAP kinase was also activated by $A\beta_{1\text{-}42}$ treatment in the cortical culture, and treatment with 4-*O*-MH dose-dependently decreased the expression of phosphorylated p38 MAP kinase (Fig. 9A). However, a 30 min pretreatment of p38 MAP kinase inhibitor U0126 (1, 2 and 5 μM) prior to the treatment of $A\beta_{1\text{-}42}$ (5 μM) abolished the protective effect of 4-*O*-MH (10 μM) on the $A\beta_{1\text{-}42}$-induced cell death (Fig. 9B).

3.6. Effect of 4-O-MH on neuronal cell death and reactive oxygen species generation in cortical neurons

ROS have been known to cause cell death and p38 MAP kinase activity, and are related with many neurodegenerative diseases. To investigate whether 4-*O*-MH could prevent cell death and block ROS generation through the prevention of the activation of p38 MAP kinase, we performed a cell viability assay and measured intracellular ROS generation induced by $A\beta_{1\text{-}42}$ in cortical neurons in the presence of 4-*O*-MH as well as p38 MAP kinase inhibitor. Treatment of $A\beta_{1\text{-}42}$ induced intracellular ROS generation, whereas 4-*O*-methylhokiol blocked $A\beta_{1\text{-}42}$-induced intracellular ROS generation in cortical neurons (Fig. 9C). However, a 30-min pretreatment of p38 MAP kinase inhibitor U0126 (1, 2 and 5 μM) prior to the treatment of $A\beta_{1\text{-}42}$ (5 μM), concentration dependently reversed the preventive effect of 4-*O*-MH on $A\beta_{1\text{-}42}$-induced ROS generation (Fig. 9C) as well as H_2O_2 (300 μM)-induced cell death (Fig. 9D).

4. Discussion

Our present results showed that 4-*O*-MH, a lignan compound isolated from *M. officinalis* improved $A\beta_{1\text{-}42}$ infusion-induced memory impairment due to the prevention of $A\beta_{1\text{-}42}$-induced neuronal cell death by the inhibition of oxidative stress and the activation of p38 MAP kinase. Oxidative stress and related signals-induced cell death were common causing mechanisms in many neurodegenerative diseases including Alzheimer's disease [43,44]. Compounds extracted from *Magnolia* family have been known to have various pharmacological actions including anti-inflammatory [31–33] and neuroprotective effects [24,25]. A recent study demonstrated that honokiol, another lignan compound extracted from *M. officinalis*, had antioxidant activity by scavenger of superoxide and peroxyl radicals [35]. In addition, honokiol and magnolol protected hepatocytes and endothelial cells against oxidative damages [45–47]. Aβ peptide in the early stages of AD is represented by the fibrillar peptide form [48]. It is well known that the aggregated Aβ is toxic in vitro to cultured neurons, finally resulting in neuronal dysfunction and death [49]. Interplay between oxidative stress and Aβ peptides has been convincingly shown as a matter of Aβ-induced neurotoxicity in vitro and in vivo [8,50–52]. We previously also demonstrated that compounds showing anti-oxidative property such as EGCG have the ability to improve memory impairment [16]. Thus, the present data showed that anti-oxidative property of 4-*O*-MH could be an important mechanism for memory enhancement capability. This hypothesis was supported by the scavenging effect of 4-*O*-MH in $A\beta_{1\text{-}42}$-induced ROS generation in cultured cortical neurons as well as reduced oxidative damages of macromolecules within the $A\beta_{1\text{-}42}$-induced mice brains.

Several lines of evidence have demonstrated that the generation of Aβ is associated with the formation of senile plaques in the brains of AD patients, which eventually cause neuronal cell death [53]. Inhibition of MAP kinase pathways has been linked to the reduction of ROS generation in Aβ-treated neuronal cell death [8,54–56]. Thus, possible signal pathway in the inhibitory effect of 4-*O*-MH on $A\beta_{1\text{-}42}$-induced neuronal cell death could be related to the inhibition of p38 MAP kinase pathway. In fact, we observed that 4-*O*-MH inhibited $A\beta_{1\text{-}42}$-induced activation p38 MAP kinase in the brain. Further in vitro study showed that the p38 MAPK kinase inhibitor abolished the inhibitory effect of 4-*O*-MH on $A\beta_{1\text{-}42}$-induced ROS generation and cell death. In this regard, it is worthy to note that obovatol, which is also a lignin compound isolated from magnolia family, inhibited the JNK and ERK signal in lipopolysaccharide (LPS)-induced nuclear

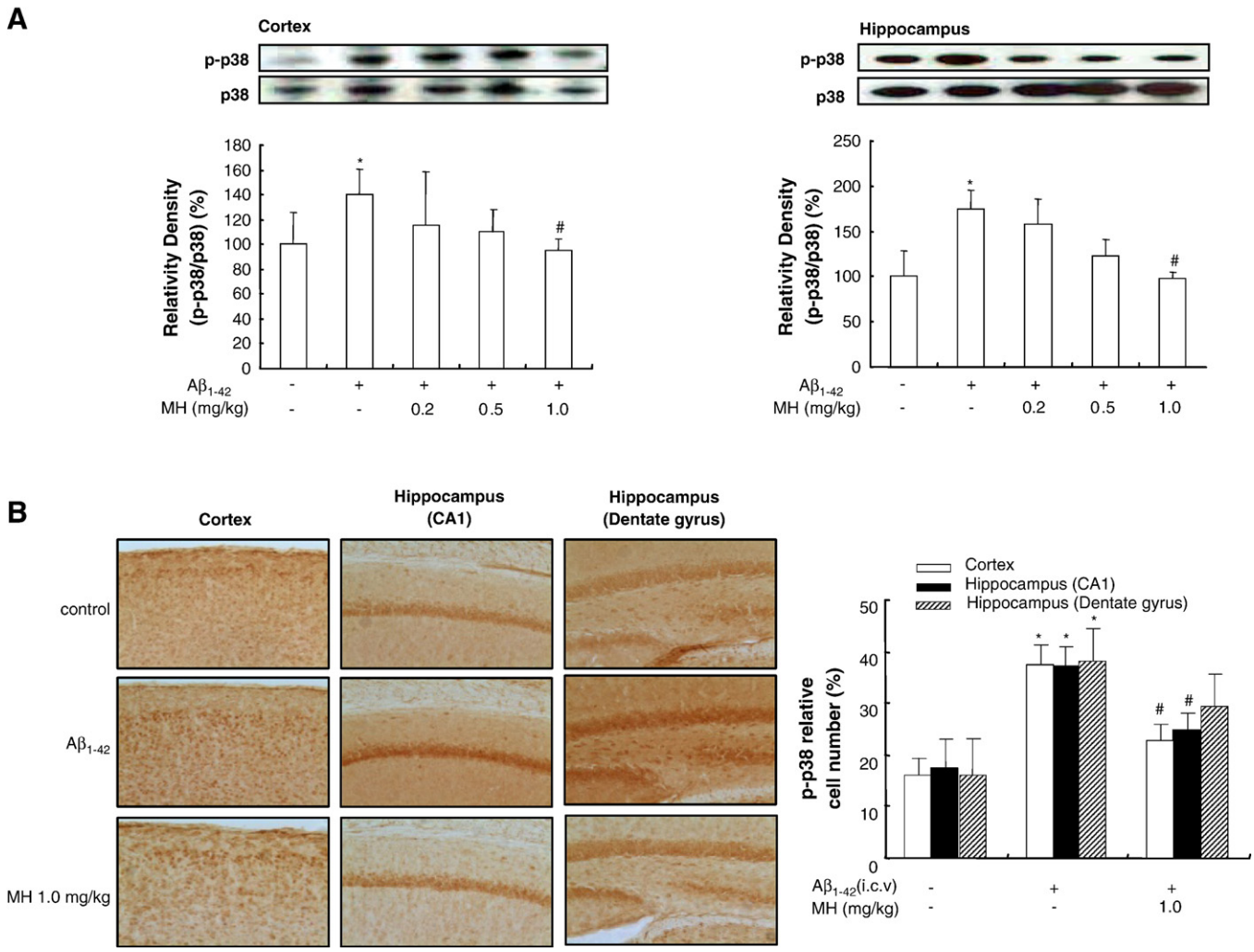

Fig. 8. Inhibitory effect of 4-*O*-MH on the $A\beta_{1\text{-}42}$-induced expression of p-p38 MAP kinase. (A) Immunoblots of lysates from brain tissue were probed with p38 and p-p38 antibodies, respectively. Experiments were performed from three mice brains. Densitometric values are the means±S.E. from three mice brains. (B) immunostaining of p-p38 in the cortex and hippocampus was performed 40 μm-thick sections of brains from mice were incubated with anti-p-p38 primary antibodies and the biotinylated secondary antibody. It was then counterstained by a hematoxylin. The resulting tissue was viewed with a microscope. A representative sample from each group was stained in the picture. The graph represents the number of p-p38 immunoreactive cells in the mice brain. All values are the means±S.E. from three mice brains. *Significantly different from vehicle control ($P<.05$). #Significantly different from $A\beta_{1\text{-}42}$ treated control ($P<.05$).

factor-κB activation and inflammation of RAW macrophages [57,58]. We recently also found that 4-*O*-MH has an anti-inflammatory effect in LPS-induced RAW 264.7 cells via inhibition of ERK activation [37]. The honokiol induced neurite outgrowth promotion depends on activation of extracellular signal-regulated kinases (ERK1/2) [55]. Even though dependence is on different stimuli and cell types, several different subtype of MAP kinase are activated by the compounds isolated from magnolia family; however, the present data suggest that 4-*O*-MH prevented $A\beta_{1\text{-}42}$-induced neuronal cell death by blocking the activation of p38 pathway in the brain.

The present study confirms the memory improving activity of 4-*O*-MH which previously showed that a suppressive effect of the oral administration of the ethanol extract of *M. officinalis* and 4-*O*-MH (1 mg/kg) against scopolamine and single injection of $A\beta_{1\text{-}42}$-induced memory impairment [39]. It is hard to predict whether such doses of MH are achievable in the brain in the absence of pharmacokinetic data. Nonetheless, it is noteworthy that the brain concentration of magnolol is fourfold higher than plasma, which suggests that 4-*O*-MH could pass through the blood brain barrier, and act on the brain [59]. The dose of 4-*O*-MH used in the present study is within the range employed in previous other studies to document neuroprotective effects of the related compounds isolated from *M. officinalis*. For instance, mice were given a single injection of 1 and 5 mg/kg of honokiol and magnolol that prevented excitatory amino acid-evoked cation signals and seizures [60]. Similar to our finding, oral treatment of more than 3 mg/kg of honokiol for 3 days ameliorated *N*-methyl-D-aspartic acid-induced oxidative damages of the mice brains [61]. Intravenous pre-treatment or post-treatment of honokiol at a concentration of 0.1 and 1.0 μm/kg significantly decreased the neutrophil infiltration and oxidative damages in the infracted infected brains [24]. It was found that dihydrohonokiol-B [3′-(2 propenyl)-5-propyl-(1,1′-biphenyl)-2,4′-diol], a partially reduced derivative of honokiol, was an effective anxiolytic-like agent in mice at an oral dose of 0.04–1 mg kg^{-1} [62]. Oral treatment of 0.2 mg/kg honokiol for seven days showed a similar anxiolytic effect with a single treatment of 1 mg kg^{-1} diazepam in mice [29]. Moreover, oral administration of 4-*O*-MH as high as 80 mg/kg dose for 4 weeks did not show weight loss or other toxicities in the 4-*O*-MH-treated mice (data not shown). It was also reported that magnolia bark extract (it may contain 10–15% of major constitutive compounds such as magnolol, honokiol, obovatol, or 4-*O*-MH) did not cause any toxic effects in rats treated with 0–480 mg/kg for 21

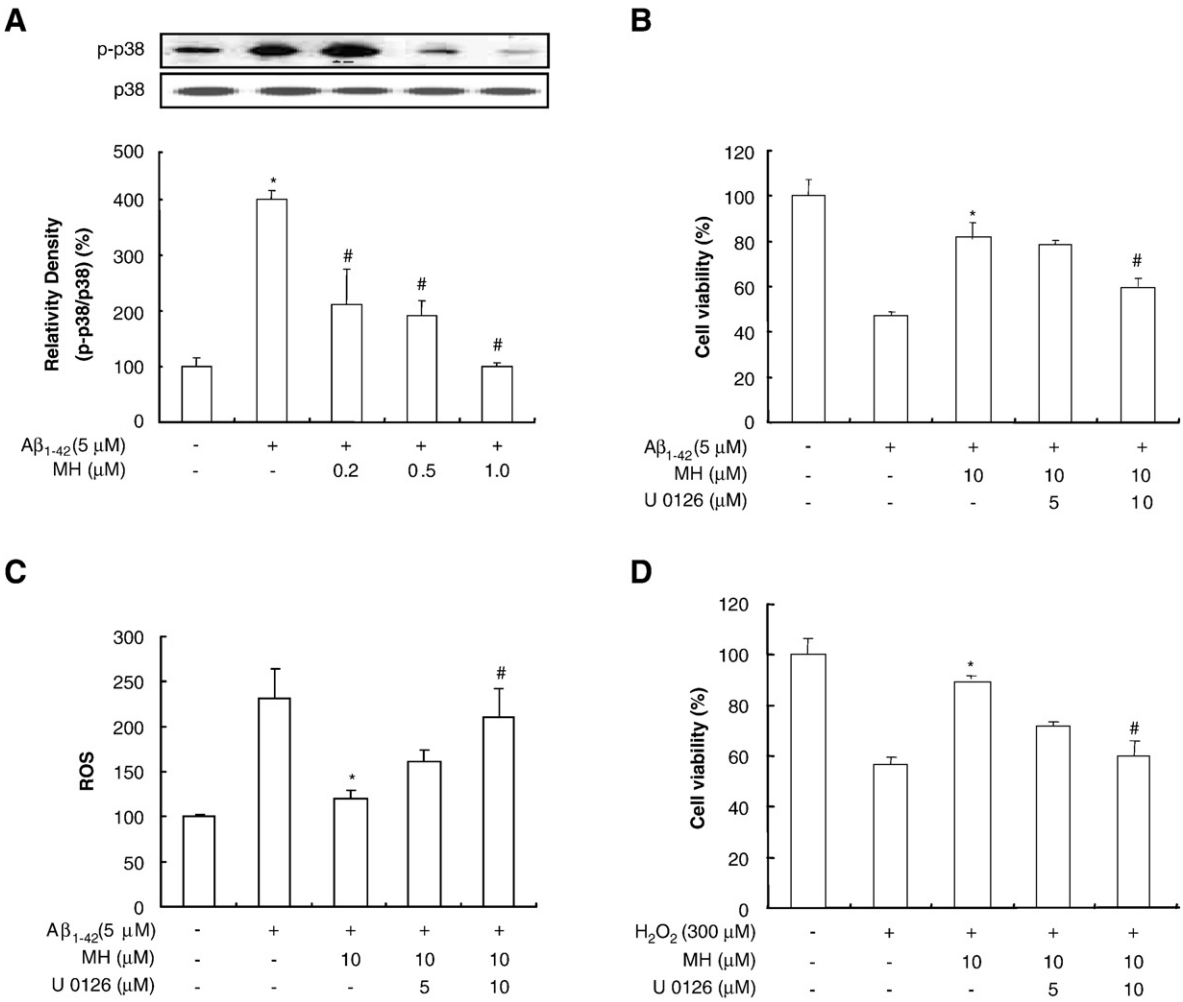

Fig. 9. Reversal effect of MAP kinase inhibitor on the prevent effect of 4-*O*-MH in the $A\beta_{1-42}$-induced cell death and ROS generation in cortical neurons. (A) Immunoblots of lysates from cortical neurons were probed with p38 and p-p38 antibodies, respectively. All values represent means±S.E. of three independent experiments performed in triplicate. (B) The cortical neurons were treated with $A\beta_{1-42}$ (5 μM), 4-*O*-MH (10 μM) and U0126 (5 and 10 μM). Cell viability was performed using the WST-1 according to the manufacturer's instructions. (C) The cortical neurons were treated with $A\beta_{1-42}$ (5 μM), 4-*O*-MH (10 μM) and U0126 (5 and 10 μM). Intracellular ROS levels were determined by measuring DCF fluorescence. (D) The cortical neurons were treated with H_2O_2 (300 μM), 4-*O*-MH (10 μM) and U0126 (5 and 10 μM). Cell viability was performed using the WST-1 according to the manufacturer's instructions. *Significantly different from vehicle control ($P<.05$). #Significantly different from $A\beta_{1-42}$ or H_2O_2-treated control ($P<.05$).

days or with 0–240 mg/kg for 90 days [64]. The dose (480 mg/kg for 3-week study, and 240 mg/kg for 90-day study) is similar to the dose (40 mg/kg) used 4 weeks treatment in our study. To further investigate whether 4-*O*-MH can have a possibility of development into an effective drug, we examined the absorption, distribution, metabolism, excretion and toxicity (ADME/Toxicity) using a prediction program (pre-ADME version 1.0.2). 4-*O*-MH has good oral and intestinal absorption as determined by the Caco-2 and MDCK cell permeability assay and was found to easily pass through the brain-blood barrier. 4-*O*-MH was also evaluated to not be rodent carcinogenicity (data not shown). These data suggest that it could be safe and effective in a clinical application. Collectively, these results suggest that 4-*O*-MH should be seriously considered for further clinical investigation to determine the possibility for prevention of development or progression of AD in humans. In summary, our data show that 4-*O*-MH has suppressed the effect against $A\beta_{1-42}$ infusion-induced memory impairment functions through the inhibition of $A\beta_{1-42}$-induced ROS generation and neuronal cell death through inactivation of p38 Map kinase. This study therefore suggests that the 4-*O*-MH may be a useful agent for the prevention of development or progression of AD.

References

[1] Weiner HL, Lemere CA, Maron R, Spooner ET, Grenfell TJ, Mori C, et al. Nasal administration of amyloid-beta peptide decreases cerebral amyloid burden in a mouse model of Alzheimer's disease. Ann Neurol 2000;48(4):567–79.
[2] Joachim CL, Selkoe DJ. The seminal role of beta-amyloid in the pathogenesis of Alzheimer disease. Alzheimer Dis Assoc Disord 1992;6(1):7–34.
[3] Cerpa W, Dinamarca MC, Inestrosa NC. Structure-function implications in Alzheimer's disease: effect of Abeta oligomers at central synapses. Curr Alzheimer Res 2008;5(3):233–43.
[4] Selkoe DJ. Presenilin, Notch, and the genesis and treatment of Alzheimer's disease. Proc Natl Acad Sci U S A 2001;98(20):11039–41.
[5] Maccioni M, Riera CM, Rivero VE. Identification of rat prostatic steroid binding protein (PSBP) as an immunosuppressive factor. J Reprod Immunol 2001;50(2):133–49.
[6] Lecanu L, Yao W, Teper GL, Yao ZX, Greeson J, Papadopoulos V. Identification of naturally occurring spirostenols preventing beta-amyloid-induced neurotoxicity. Steroids 2004;69(1):1–16.
[7] Hwang DY, Chae KR, Kang TS, Hwang JH, Lim CH, Kang HK, et al. Alterations in behavior, amyloid beta-42, caspase-3, and Cox-2 in mutant PS2 transgenic mouse model of Alzheimer's disease. FASEB J 2002;16:805–13.
[8] Lee SY, Hwang DY, Kim YK, Lee JW, Shin IC, Oh KW, et al. PS2 mutation increases neuronal cell vulnerability to neurotoxicants through activation of caspase-3 by enhancing of ryanodine receptor-mediated calcium release. FASEB J 2006;20:151–3.
[9] Feld M, Galli C, Piccini A, Romano A. Effect on memory of acute administration of naturally secreted fibrils and synthetic amyloid-beta peptides in an invertebrate model. Neurobiol Learn Mem 2008;89(4):407–18.

[10] Repici M, Zanjani HS, Gautheron V, Borsello T, Dusart I, Mariani J. Specific JNK inhibition by D-JNKI1 protects Purkinje cells from cell death in Lurcher mutant mouse. Cerebellum 2008;7(4):534–8.
[11] Chen HS, He X, Qu F, Kang SM, Yu Y, Liao D, et al. Differential roles of peripheral mitogen-activated protein kinase signal transduction pathways in bee venom-induced nociception and inflammation in conscious rats. J Pain 2009;10(2): 201–7.
[12] Munoz L, Ranaivo HR, Roy SM, Hu W, Craft JM, McNamara LK, et al. A novel p38 alpha MAPK inhibitor suppresses brain proinflammatory cytokine up-regulation and attenuates synaptic dysfunction and behavioral deficits in an Alzheimer's disease mouse model. J Neuroinflammation 2007;4:21.
[13] Zhu Y, Hou H, Nikolic WV, Ehrhart J, Rrapo E, Bickford P, et al. CD45RB is a novel molecular therapeutic target to inhibit Abeta peptide-induced microglial MAPK activation. PLoS One 2008;3(5):e2135.
[14] Origlia N, Righi M, Capsoni S, Cattaneo A, Fang F, Stern DM, et al. Receptor for advanced glycation end product-dependent activation of p38 mitogen-activated protein kinase contributes to amyloid-beta-mediated cortical synaptic dysfunction. J Neurosci 2008 Mar 26;28(13):3521–30.
[15] Song YS, Park HJ, Kim SY, Lee SH, Yoo HS, Lee HS, et al. Protective role of Bcl-2 on beta-amyloid-induced cell death of differentiated PC12 cells: reduction of NF-kappaB and p38 MAP kinase activation. Neurosci Res 2004; 49(1):69–80.
[16] Lee JW, Lee YK, Ban JO, Ha TY, Yun YP, Han SB, et al. Green tea (−)-epigallocatechin-3-gallate inhibits beta-amyloid-induced cognitive dysfunction through modification of secretase activity via inhibition of ERK and NF-kappaB pathways in mice. J Nutr 2009;139(10):1987–93.
[17] Lee SY, Lee JW, Lee HS, Yoo HS, Yun YP, Oh KW, et al. Inhibitory effect of green tea extract on β-amyloid-induced PC12 cell death by inhibition of the activation of NF-κB and ERK/p38 MAP kinase pathway through antioxidant mechanisms. Mol Brain Res 2005;140:45–54.
[18] Butterfield DA. Amyloid beta-peptide (1-42)-induced oxidative stress and neurotoxicity: implications for neurodegeneration in Alzheimer's disease brain. A review. Free Radic Res 2002;36(12):1307–13.
[19] Jang JH, Surh YJ. beta-Amyloid induces oxidative DNA damage and cell death through activation of c-Jun N terminal kinase. Ann N Y Acad Sci 2002;973:228–36.
[20] Dumont M, Wille E, Stack C, Calingasan NY, Beal MF, Lin MT. Reduction of oxidative stress, amyloid deposition, and memory deficit by manganese superoxide dismutase overexpression in a transgenic mouse model of Alzheimer's disease. FASEB J 2009;23(8):2459–66.
[21] Montiel T, Camacho A, Estrada-Sánchez AM, Massieu L. Differential effects of the substrate inhibitor l-trans-pyrrolidine-2,4-dicarboxylate (PDC) and the non-substrate inhibitor DL-threo-beta-benzyloxyaspartate (DL-TBOA) of glutamate transporters on neuronal damage and extracellular amino acid levels in rat brain in vivo. Neuroscience 2005;133(3):667–78.
[22] Arias C, Montiel T, Quiroz-Báez R, Massieu L. beta-Amyloid neurotoxicity is exacerbated during glycolysis inhibition and mitochondrial impairment in the rat hippocampus in vivo and in isolated nerve terminals: implications for Alzheimer's disease. Exp Neurol 2002;176(1):163–74.
[23] Yatin SM, Varadarajan S, Butterfield DA. Vitamin E prevents Alzheimer's amyloid beta-peptide (1-42)-induced neuronal protein oxidation and reactive oxygen species production. J Alzheimers Dis 2000;2(2):123–31.
[24] Liou KT, Shen YC, Chen CF, Tsao CM, Tsai SK. Honokiol protects rat brain from focal cerebral ischemia-reperfusion injury by inhibiting neutrophil infiltration and reactive oxygen species production. Brain Res 2003;992(2):159–66.
[25] Lin YR, Chen HH, Ko CH, Chan MH. Neuroprotective activity of honokiol and magnolol in cerebellar granule cell damage. Eur J Pharmacol 2006;537(1-3):64–9.
[26] Frank B, Gupta S. A review of antioxidants and Alzheimer's disease. Ann Clin Psychiatry 2005;17(4):269–86.
[27] Rezai-Zadeh K, Arendash GW, Hou H, Fernandez F, Jensen M, Runfeldt M, et al. Green tea epigallocatechin-3-gallate (EGCG) reduces beta-amyloid mediated cognitive impairment and modulates tau pathology in Alzheimer transgenic mice. Brain Res 2008;1214:177–87.
[28] Kim TI, Lee YK, Park SG, Choi IS, Ban JO, Park HK, et al. l-Theanine, an amino acid in green tea, attenuates beta-amyloid-induced cognitive dysfunction and neurotoxicity: reduction in oxidative damage and inactivation of ERK/p38 kinase and NF-kappaB pathways. Free Radic Biol Med 2009;47:1601–10.
[29] Kuribara H, Stavinoha WB, Maruyama Y. Behavioural pharmacological characteristics of honokiol, an anxiolytic agent present in extracts of Magnolia bark, evaluated by an elevated plus-maze test in mice. J Pharm Pharmacol 1998;50(7): 819–26.
[30] Watanabe K, Watanabe H, Goto Y, Yamaguchi M, Yamamoto N, Hagino K. Pharmacological properties of magnolol and honokiol extracted from *Magnolia officinalis*: central depressant effects. Planta Med 1983;49(2):103–8.
[31] Zhou HY, Shin EM, Guo LY, Youn UJ, Bae K, Kang SS, et al. Anti-inflammatory activity of 4-methoxyhonokiol is a function of the inhibition of iNOS and COX-2 expression in RAW 264.7 macrophages via NF-kappaB, JNK and p38 MAPK inactivation. Eur J Pharmacol 2008;586(1-3):340–9.
[32] Munroe ME, Arbiser JL, Bishop GA. Honokiol, a natural plant product, inhibits inflammatory signals and alleviates inflammatory arthritis. J Immunol 2007;179 (2):753–63.
[33] Lin YR, Chen HH, Ko CH, Chan MH. Effects of honokiol and magnolol on acute and inflammatory pain models in mice. Life Sci 2007;81(13):1071–8.
[34] Fujita S, Taira J. Biphenyl compounds are hydroxyl radical scavengers: their effective inhibition for UV-induced mutation in *Salmonella typhimurium* TA102. Free Radic Biol Med 1994;17(3):273–7.
[35] Dikalov S, Losik T, Arbiser JL. Honokiol is a potent scavenger of superoxide and peroxyl radicals. Biochem Pharmacol 2008;76(5):589–96.
[36] Chen CL, Chang PL, Lee SS, Peng FC, Kuo CH, Chang HT. Analysis of magnolol and honokiol in biological fluids by capillary zone electrophoresis. J Chromatogr A 2007;1142(2):240–4.
[37] Oh JH, Kang LL, Ban JO, Kim YH, Kim KH, Han SB, et al. Anti-inflammatory effect of 4-*O*-MH, a novel compound isolated from *Magnolia officinalis* through inhibition of NF-kappaB. Chem Biol Interact 2009;180(3):506–14.
[38] Lee YK, Choi IS, Kim YH, Kim KH, Nam SY, Yun YW, et al. Neurite outgrowth effect of 4-*O*-MH by induction of neurotrophic factors through ERK activation. Neurochem Res 2009;34:2251–60.
[39] Lee YK, Yuk DY, Kim TI, Kim YH, Kim KT, Kim KH, et al. Protective effect of the ethanol extract of Magnolia officinalis and 4-*O*-MH on scopolamine-induced memory impairment and the inhibition of acetylcholinesterase activity. Nat Med (Tokyo) 2009;63(3):274–82.
[40] Nabeshima T, Nitta A. Memory impairment and neuronal dysfunction induced by beta-amyloid protein in rats. Tohoku J Exp Med 1994;174(3):241–9.
[41] Frautschy SA, Hu W, Kim P, Miller SA, Chu T, Harris-White ME, et al. Phenolic anti-inflammatory antioxidant reversal of Abeta-induced cognitive deficits and neuropathology. Neurobiol Aging 2001;22(6):993–1005.
[42] Morris R. Developments of water-maze procedure for studying spatial learning in the rat. J Neurosci Methods 1984;11:47–60.
[43] Gibson GE, Zhang H. Abnormalities in oxidative processes in non-neuronal tissues from patients with Alzheimer's disease. J Alzheimers Dis 2001;3(3):329–38.
[44] Finkel T, Holbrook NJ. Oxidants, oxidative stress and the biology of ageing. Nature 2000;408(6809):239–47.
[45] Chiu JH, Ho CT, Wei YH, Lui WY, Hong CY. In vitro and in vivo protective effect of honokiol on rat liver from peroxidative injury. Life Sci 1997;61(19):1961–71.
[46] Ou HC, Chou FP, Lin TM, Yang CH, Sheu WH. Protective effects of honokiol against oxidized LDL-induced cytotoxicity and adhesion molecule expression in endothelial cells. Chem Biol Interact 2006;161(1):1–13.
[47] Ou HC, Chou FP, Sheu WH, Hsu SL, Lee WJ. Protective effects of magnolol against oxidized LDL-induced apoptosis in endothelial cells. Arch Toxicol 2007;81(6): 421–32.
[48] Drouet B, Pinçon-Raymond M, Chambaz J, Pillot T. Molecular basis of Alzheimer's disease. Cell Mol Life Sci 2000;57(5):705–15.
[49] Yankner BA. Mechanisms of neuronal degeneration in Alzheimer's disease. Neuron 1996;16(5):921–32.
[50] Harkany T, Abrahám I, Kónya C, Nyakas C, Zarándi M, Penke B, et al. Mechanisms of beta-amyloid neurotoxicity: perspectives of pharmacotherapy. Rev Neurosci 2000;11(4):329–82 [Review].
[51] Behl C, Davis JB, Lesley R, Schubert D. Hydrogen peroxide mediates amyloid beta protein toxicity. Cell 1994;77(6):817–27.
[52] Yatin SM, Aksenova M, Aksenov M, Markesbery WR, Aulick T, Butterfield DA. Temporal relations among amyloid beta-peptide-induced free-radical oxidative stress, neuronal toxicity, and neuronal defensive responses. J Mol Neurosci 1998; 11(3):183–97.
[53] Borchelt DR, Ratovitski T, van Lare J, Lee MK, Gonzales V, Jenkins NA, et al. Accelerated amyloid deposition in the brains of transgenic mice coexpressing mutant presenilin 1 and amyloid precursor proteins. Neuron 1997;19:939–45.
[54] Wasilewska-Sampaio AP, Silveira MS, Holub O, Goecking R, Gomes FC, Neto VM, et al. Neuritogenesis and neuronal differentiation promoted by 2,4-dinitrophenol, a novel anti-amyloidogenic compound. FASEB J 2005;19(12): 1627–36.
[55] Marques CA, Keil U, Bonert A, Steiner B, Haass C, Muller WE, et al. Neurotoxic mechanisms caused by the Alzheimer's disease-linked Swedish amyloid precursor protein mutation: oxidative stress, caspases, and the JNK pathway. J Biol Chem 2003;278(30):28294–302.
[56] Ekinci FJ, Malik KU, Shea TB. Activation of the L voltage-sensitive calcium channel by mitogen-activated protein (MAP) kinase following exposure of neuronal cells to beta-amyloid. MAP kinase mediates beta-amyloid-induced neurodegeneration. J Biol Chem 1999;274(42):30322–7.
[57] Choi MS, Lee SH, Cho HS, Kim Y, Yun YP, Jung HY, et al. Inhibitory effect of obovatol on nitric oxide production and activation of NF-kappaB/MAP kinases in lipopolysaccharide-treated RAW 264.7cells. Eur J Pharmacol 2007;556(1-3): 181–9.
[58] Zhai H, Nakade K, Oda M, Mitsumoto Y, Akagi M, Sakurai J, et al. Honokiol-induced neurite outgrowth promotion depends on activation of extracellular signal-regulated kinases (ERK1/2). Eur J Pharmacol 2005;516(2):112–7.
[59] Tsai TH, Chou CJ, Chen CF. Pharmacokinetics and brain distribution of magnolol in the rat after intravenous bolus injection. J Pharm Pharmacol 1996;48(1): 57–9.
[60] Lin YL, Chen HH, Ko CH, Chan MH. Differential inhibitory effect of honokiol and magnolol on excitatory amino acid-evoked cation signals and NMDA-induced seizures. J Neuropharm 2005;542:550–8.
[61] Cui HS, Huang LS, Sok DE, Shin J, Kwon BM, Youn UJ, et al. Protective action of honokiol, administered orally, against oxidative stress in brain of mice challenged with NMDA. (1–100 mg/kg 3days). Phytomedicine 2007;14(10): 696–700.
[62] Maruyama Y, Kuribara H, Kishi E, Weintraub ST, Ito Y. Confirmation of the anxiolytic-like effect of dihydrohonokiol following behavioural and biochemical assessments. J Pharm Pharmacol 2001;53(5):721–5.
[64] Liu Z, Zhang X, Cui W, Zhang X, Li N, Chen J, et al. Evaluation of short-term and subchronic toxicity of magnolia bark extract in rats. Regul Toxicol Pharmacol 2007;49(3):160–71.